

PLANETESIMAL DYNAMICS IN INCLINED BINARY SYSTEMS: THE ROLE OF GAS-DISK GRAVITY

GANG ZHAO¹, JI-WEI XIE^{*1,2}, JI-LIN ZHOU¹ AND DOUGLAS N.C. LIN^{3,4}

¹Department of Astronomy & Key Laboratory of Modern Astronomy and Astrophysics in Ministry of Education, Nanjing University, Nanjing, China 210093.

²Department of Astronomy and Astrophysics, University of Toronto, Toronto, ON M5S 3H4, Canada;

³UCO/Lick Observatory, University of California, Santa Cruz, CA 95064 and

⁴Kavli Institute for Astronomy and Astrophysics, Peking University, Beijing, China

Draft version October 31, 2018

ABSTRACT

We investigate the effects of gas-disk gravity on the planetesimal dynamics in inclined binary systems, where the circumprimary disk plane is tilted by a significant angle (i_B) with respect to the binary disk plane. Our focus is on the Lidov-Kozai mechanism and the evolution of planetesimal eccentricity and inclination. Using both analytical and numerical methods, we find that, on one hand, the disk gravity generally narrows down the Kozai-on region, i.e., the Lidov-Kozai effect can be suppressed in certain parts of (or even the whole of) the disk, depending on various parameters. In the Kozai-off region, planetesimals would move on orbits close to the mid-plane of gas-disk, with the relative angle (i') following a small amplitude periodical oscillation. On the other hand, when we include the effects of disk gravity, we find that the Lidov-Kozai effect can operate even at arbitrarily low inclinations (i_B), although lower i_B leads to a smaller Kozai-on region. Furthermore, in the Kozai-on region, most planetesimals' eccentricities can be excited to extremely high values (~ 1), and such extreme high eccentricities usually accompany orbital flipping, i.e., planetesimal orbit flips back and forth between antegrade and retrograde. Once a planetesimal reaches very high orbital eccentricity, gas drag damping will shrink the planetesimal orbit, forming a "hot planetesimal" on a near circular orbit very close to the primary star. Such a mechanism, if replacing the planetesimals and gas drag damping with Jupiters and tidal damping respectively, may lead to frequent production of hot-Jupiters..

Subject headings: Celestial mechanics - planetary systems: formation

1. INTRODUCTION

As of today, over 60 exoplanets have been found in binary star systems, and current observations show that the multiplicity rate of the detected exoplanet host stars is around 17% (Mugrauer & Neuhäuser 2009; Eggenberger 2010). Planet formation in binary system systems presents numerous challenges, as each stage of the planet formation process can be affected by the binary companion. A crucial stage that may be particularly sensitive to binary effects is the accumulation of 1-100 km-sized planetesimals (see the review by Haghighipour (2010) and the references therein). Because of the perturbations from the binary companion, planetesimals will be excited to orbits with high relative velocities, preventing or even ceasing their growth (Heppenheimer 1978; Whitmire et al. 1998). In the past decade, with several discoveries of exoplanets in close binary of separation ~ 20 AU (Queloz et al. 2000; Hatzes et al. 2003; Zucker et al. 2004; Correia et al. 2008; Chauvin et al. 2011), the issue of planetesimal growth in binary systems becomes more challenging and therefore attracts many researchers as well as many dynamical and collisional studies (Marzari & Scholl 2000; Moriwaki & Nakagawa 2004; Thébault et al. 2004, 2006, 2008, 2009; Thébault 2011; Paardekooper et al. 2008; Scholl et al. 2007; Paardekooper & Leinhardt 2010; Kley & Nelson 2008; Beaugé et al. 2010; Giuppone et al. 2011; Xie & Zhou 2008, 2009; Xie et al. 2010a,b).

Most of previous studies had considered only coplanar or near-coplanar cases, where the tilted angle between the binary orbital plane and the circumprimary disk plane was close to zero, i.e., $i_B \sim 0$. In fact, the coplanar case is reasonable only if it is applied to relatively close binary systems with

separation less than ~ 40 -200 AU (Hale 1994; Jensen et al. 2004), beyond which the distribution of i_B is likely to be random and therefore the highly inclined case is more relevant. Planetesimal dynamics in highly inclined binary systems have only been investigated by Marzari et al. (2009b), and most recently (at the time of writing this paper) by Xie et al. (2011), Fragner et al. (2011), and Batygin et al. (2011).

Marzari et al. (2009b) found that, due to the perturbations of a inclined binary companion, planetesimals' nodal lines became progressively randomized, raising their relative velocities to the degree that planetesimal growth by mutual collision was significantly prevented. Nevertheless, the gaseous protoplanetary disk was ignored in their study, where planetesimals were only subject to the gravity of the binary stars. In reality, the gaseous disk can generally have crucial effects on planetesimal dynamics through two factors. One is the hydrodynamic drag force, which has been investigated in detail by Xie et al. (2011). When gas drag is included, it is found that planetesimals from the outer regions (where conditions are hostile to planetesimal accretion) jump inward into an accretion-friendly region and pile-up there. This is referred to as the planetesimal jumping-piling effect (PJP), and its general result, as shown in Xie et al. (2011), is to form a severely truncated and dense planetesimal disk around the primary, providing conditions which are favorable for planetesimal growth and potentially allow for the subsequent formation of planets. Another crucial factor is the gravity of gaseous disk, which has been studied recently by Fragner et al. (2011) with a hydro-dynamical model and by Batygin et al. (2011) with an analytical model. Generally, it is found that the gravity could pull the planetesimals back towards the middle plane of gas-disk. With proper conditions, such as a massive gas disk and/or a large binary distance, Lidov-Kozai effect could

* Corresponding to xiejawei@gmail.com

be suppressed regardless of i_B . However, Fragner et al. (2011) could only focus on several typical cases with a few planetesimals in relative short simulation timescale because of the large computational hours, while Batygin et al. (2011) only concentrated on cases of very wide binaries with separation of ~ 1000 AU, aiming to just identify the important physical processes at play.

In this paper, we investigate the effects of gas-disk gravity on planetesimal dynamics in inclined binary systems through both analytical and numerical fashions. Analytically, we derived the condition at which Lidov-Kozai effect is turned off by the disk gravity. Numerically, we confirm our analytical results and provide a global quantitative view of the role of gas-disk gravity in a large parameter space. Furthermore, one specific attention is given to the role of disk gravity in shaping the PJP effect found by Xie et al. (2011). The paper is outlined as follows.

In section 2, we describe our disk model and the initial set up. In section 3, we analyze the secular motion of a planetesimal under the gravity of disk and stars, focusing on the evolution of planetesimal inclination and eccentricity. The analytical study is followed by the numerical simulations presented in section 4. In section 5, we discuss some issues, including the PJP effect, implication for hot-Jupiters and disk precession. Then in Section 6 we present our summary.

2. DISK MODEL

In our model, planetesimals are assumed to be initially moving on circular orbits in the mid-plane² of a gaseous disk around the central star with one solar mass (M_\odot). A companion star with mass of M_B (a free parameter) is orbiting around the central star-disk system with an orbital semimajor axis of a_B (a free parameter), inclination of i_B (a free parameter, relative to the mid-plane of the disk), eccentricity of $e_B = 0$ (constant). In this paper, for simplicity, we only consider the circular case ($e_B = 0$) and focus on the effect of gas gravity. For the eccentric case $e_B \neq 0$, the Lidov-Kozai mechanism itself is more complicated (Katz et al. 2011; Lithwick & Naoz 2011), and thus this case³ is not addressed in this paper.

For the gas disk, we use a 3-dimension steady model as in Takeuchi & Lin (2002). In cylindrical coordinates (r, z) , the disk density profile is

$$\rho_g(r, z) = \rho_0 f_g \left(\frac{r}{\text{AU}} \right)^\beta \exp\left(-\frac{z^2}{2h_g^2}\right), \quad (1)$$

and the gas rotation rate is

$$\Omega_g(r, z) = \Omega_{\text{K,mid}} \left[1 + \frac{1}{2} \left(\frac{h_g}{r} \right)^2 \left(\beta + \gamma + \frac{\gamma z^2}{2h_g^2} \right) \right], \quad (2)$$

where $\Omega_{\text{K,mid}}$ is the Keplerian rotation in the mid-plane, $h_g(r) = h_0(r/\text{AU})^{(\gamma+3)/2}$ is the scale height of gas disk, f_g is a scaling number with respect to the minimum mass of solar nebulae (Hayashi (1981), MMSN hereafter), $\rho_0 = 2.83 \times 10^{-10} \text{gcm}^{-3}$, $\gamma = -0.5$, $h_0 = 0.33 \times 10^{-2}$, and β is a free

² This is equivalent to assume that their proper eccentricities (and inclinations) are equal to the forced one.

³ If $e_B = 0$, the average Hamiltonian is axisymmetric, thus the vertical angular momentum is an integral of motion, and the planetesimal orbit can be well described with the classic Kozai effect. Otherwise, if $e_B > 0$, the vertical angular momentum is not a constant any more, and the classic Kozai effect should be modified with the so called Eccentric Kozai effect (Lithwick & Naoz 2011).

parameter. The surface density of the disk has a power-law form of $\Sigma_g = \sqrt{2\pi}\rho_0 f_g h_0 (r/\text{AU})^k$, where $k = \beta + 1.25$. Normally, in this paper, we set $k = -1$ as the stander case. The inner and outer boundaries of the disk are set as $r_{\text{in}} = 0.1$ AU and $r_{\text{out}} = 12.5$ AU. Their values have little effect on the final results as long as they are not very close to the planetesimals.

Our disk model is a very simple one, which ignores the reaction of gas disk to the binary perturbations. In more realistic situations, as shown in the simulations of Larwood et al. (1996); Fragner & Nelson (2010), the disk will become eccentric, develop a warp and precess under the perturbations of the companion star. Nevertheless, as pointed out by Fragner et al. (2011) (also see our discussion in section 5.2), planetesimals' secular dynamical behaviors are similar both in the evolving and non-evolving disk models, and thus our choice of a steady model can be reasonable to at least a zeroth order approximation. Furthermore, using such a simple gas disk model is much less time consuming in computing the disk gravity as compared to using a hydrodynamical code, allowing us to see the effect of disk gravity on a much longer timescale. In addition, our simple gas disk model is convenient for making some analytical studies.

It also worthy noting that the gaseous disk would slowly relax to the binary orbital plane on the viscous evolution timescale (Fragner & Nelson 2010). Thus the assumption of a constant and relatively large i_B in our model is only relevant if the viscous timescale, $t_{\text{vis}} \sim r^2 / (ah^2 \Omega_{\text{K,mid}})$, is larger than the secular perturbation timescale, $t_{\text{sec}} \sim 2\pi/B$. Equating these two timescales, the critical viscous parameter can be derived as

$$\alpha_c \sim 5 \times 10^{-2} \left(\frac{r}{10\text{AU}} \right)^{5/2} \left(\frac{a_B}{50\text{AU}} \right)^{-3} \left(\frac{M_B}{M_\odot} \right)^{1/2}. \quad (3)$$

Therefore, a high inclined case, which studied in this paper, is relevant only for $\alpha < \alpha_c$. If otherwise, $\alpha > \alpha_c$, it is likely to reduce to a near coplanar case, which has been studied in many previous works (Marzari & Scholl 2000; Thébault et al. 2006; Paardekooper et al. 2008; Xie & Zhou 2008, 2009).

3. ANALYTIC STUDY

In this section, we analytically study the secular dynamics of a planetesimal under the gravitational perturbations from both the companion star and the disk. Our interests focus on the evolution of the planetesimal's orbital eccentricity and inclination, aiming to see how the Lidov-Kozai effect operates if the disk gravity is included. For the sake of this derivation, we introduce two coordinate systems: (1) the disk coordinate, where the $X'Y'$ -plane is set as the disk mid-plane with the X' direction towards the ascending node of the binary orbit, and (2) the binary coordinate, where the XY -plane is set as the orbital plane of the binary star with the X direction the same as X' . In the disk coordinate system, angular elements are marked with a superscript (" $'$ "). For example, i' and Ω' denote the orbital inclination and longitude of ascending node in the disk coordinate system respectively, while i and Ω are those in the binary coordinate system.

3.1. The Disturbing Function

The disturbing function of the star-disk-planet system can be expressed as

$$R = R_D + R_B, \quad (4)$$

where R_D and R_B are contributions from the gravity of disk and binary stars, respectively.

According to Nagasawa et al. (2000) (see the appendix of their paper), taking the second order approximation, R_D can be expressed as

$$R_D = -\frac{na^2}{2} [Te^2 + Si'^2], \quad (5)$$

where n , a , e and i' are the orbital mean frequency, semi-major axis, eccentricity, inclination (in disk coordinate) of the planetesimal. T and S are two characteristic frequencies (see the appendix of this paper for details of their definition and calculation) which, under the disk model assumed in section 2, can be approximately fit by the following formulas.

$$T(a) = f_g \times 4.5 \times 10^{-4} \left(\frac{a}{\text{AU}}\right)^{k+1} \text{ rad/yr}, \quad (6)$$

$$S(a) = f_g \times 1.7 \times 10^{-2} \left(\frac{a}{\text{AU}}\right)^{k+1/4} \text{ rad/yr}.$$

Note, T is actually the apsidal recession rate of a planetesimal if the planetesimal is affected only by the disk gravity in the coplanar case ($i' = 0$). Our calculation of T is generally consistent with that of Batygin et al. (2011) (here $f_g = 1$ corresponds to a disk mass of $\sim 0.02M_\odot$ in the figure 2 of their paper) who used a similar disk model but different computing technics. However, we emphasize that T should be scaled with the local surface density as in equation (6) rather than with the total mass of the disk (as was done in figure 2 of Batygin et al. (2011) and Eqn. (30) in Fragner et al. (2011)).

Following Innanen et al. (1997), the binary part of the disturbing function can be expressed as:

$$R_B = \frac{na^2}{2} B [e^2 - (1 + 4e^2 - 5e^2 \cos^2 \omega) \sin^2 i], \quad (7)$$

where i and ω denote the orbital inclination and pericenter (in binary coordinate) of the planetesimal. The characteristic frequency B is actually the precession rate of the planetesimal caused by the secular binary perturbation in the coplanar case ($i = 0$), and in the first order it can be expressed as

$$B \sim B_1 = \frac{3GM_B}{4na_B^3(1 - e_B^2)^{3/2}}. \quad (8)$$

However, such a first order expression can be rather inaccurate unless one uses the second order correction (B_2) as suggested by Thébault et al. (2006) and Giuppone et al. (2011),

$$B \sim B_2 = B_1 \left[1 + \frac{32M_B}{M(1 - e_B^2)^3} \left(\frac{a}{a_B}\right)^2 \right]. \quad (9)$$

Hereafter, we adopt $B = B_2$ if there is no specific explanation.

We plot T , S , and B in Figure 1 for the standard case, where the companion has mass of $M_B = 0.5M_\odot$, semimajor axis of $a_B = 50$ AU, and the disk surface density slope of $k = -1$. The blue dotted line, red dashed line, and black solid line indicate T , S and B as a function of the semimajor axis of the planetesimal (a), respectively. As can be seen, S is much greater than T and B in the whole of the plotted region of the disk, while T is greater (less) than B in the inner (outer) region. We will show in the following subsections that such a picture of T , B and S determines the dynamical evolution of the planetesimal's orbit.

3.2. Evolution of the Planetesimal Inclination

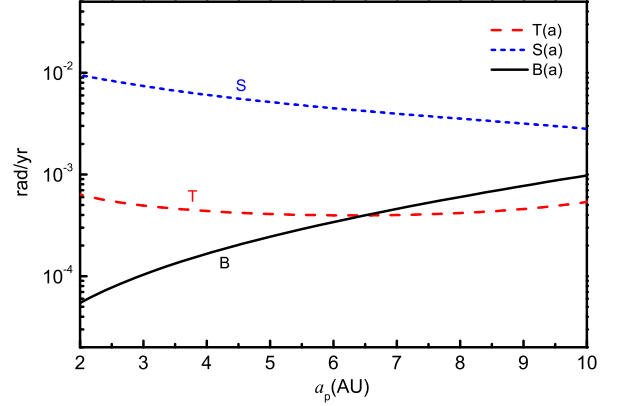


FIG. 1.— The values of $T(a)$, $S(a)$, and $B(a)$. The blue dotted line and red dashed line indicate $T(a)$ and $S(a)$ of an MMSN disk with inner edge 0.1AU and outer edge 12.5AU and surface density slope of $k = -1$. The black solid line shows $B(a)$ of a companion star at $a_B = 50$ AU with $0.5M_\odot$.

As the planetesimal is initially moving on a circular orbit in the mid-plane of the disk, the initial e and i' are approximately zero, thus we ignore quantities that are on an order of higher than $o(e^2)$, $o(i'^2)$ or $o(ei')$. The disturbing function relating to the inclination then can be reduced to

$$R_{rd} \sim \frac{na^2}{2} [-Si'^2 - B \sin^2 i]. \quad (10)$$

Considering the relation between i , i' and Ω' and introducing two new variables $p = i' \sin \Omega'$ and $q = i' \cos \Omega'$, then Lagrange's planetary equations (relating to i' and Ω') can be written as (see the appendix for detailed derivation)

$$\begin{aligned} \frac{dp}{dt} &= -(B \cos 2i_B + S) q + \frac{B}{2} \sin 2i_B, \\ \frac{dq}{dt} &= (B \cos^2 i_B + S) p, \end{aligned} \quad (11)$$

where i_B is the angle between the disk plane and the binary orbital plane. Note $S > B > 0$ and the initial condition $p_0 = q_0 = 0$, thus the solution of p and q can be written as

$$\begin{aligned} p &= \frac{B \sin(2i_B)}{2f} \sin(ft), \\ q &= \frac{B \sin(2i_B)}{2B \cos 2i_B + 2S} [1 - \cos(ft)], \end{aligned} \quad (12)$$

where $f = \sqrt{(B \cos^2 i_B + S)(B \cos 2i_B + S)}$. The maximum value of i' (note that $i' = \sqrt{p^2 + q^2}$) is

$$i'_{\max} = \frac{B \sin(2i_B)}{B \cos 2i_B + S}. \quad (13)$$

As $S \gg B$ shown in Figure 1, thus $f \sim S$ and i'_{\max} is as small as on an order of $o(B/S)$. It means that the planetesimal will keep its orbital plane close to the disk mid-plane, having the relative titled angle i' oscillating with a frequency of $f \sim S$ and an amplitude of $\sim B/S$. Such an analytical result is consistent with the hydrodynamical simulation performed by Fragner et al. (2011), which has shown that the disk gravity

would try to pull the planetesimal orbit back to the disk mid-plane, maintaining a small relative angle (see the figures 3 and 10 in their paper).

Recalling the approximation (quantities that are $O(e^2)$, $O(i^2)$ or $O(ei)$ or higher are ignored) adopted before our derivation, we thus emphasize that our analytical results about the evolution of planetesimal inclination remain valid only if the planetesimal eccentricity is not excited or remains at a low value. Such an assumption, however, will break down if the Lidov-Kozai effect kicks in. In the following subsection, we will address this issue, deriving the conditions in which the Lidov-Kozai effect takes over and planetesimal eccentricity is excited.

3.3. Evolution of the Planetesimal Eccentricity

Following Innanen et al. (1997), the Lagrange planetary equations describing the evolution of the planetesimal's orbital eccentricity (e) and pericenter (ω) can be written as

$$\frac{de}{dt} \sim \frac{5B}{2} e \sin(2\omega) \sin^2 i_B \quad (14)$$

$$\frac{d\omega}{dt} \sim B(2 - 5 \sin^2 \omega \sin^2 i_B) + D. \quad (15)$$

Compared to the equation (5) in the paper of Innanen et al. (1997), here we add the term of contribution from the disk (D), ignore quantities that are on an order of $o(e^2)$ or higher because of the initial circular planetesimal orbit, and take $i \sim i_B$ because i' is very small before e is excited according to equation (13). The disk contribution term (D) can be written as (see the appendix for the detail of derivation)

$$D \sim -T - \frac{SB \cos^2 i_B}{B \cos 2i_B + S}. \quad (16)$$

Note⁴, as $i = 0$ is a singular point in the Lagrange planetary equation, thus equation (15) and (16) cannot be applied to the case of $i_B = 0$.

For the Lidov-Kozai effect to kick in, we expect $d\omega/dt \approx 0$. Using this condition to eliminate the variable ω in equations (15) and (16), we then have,

$$\frac{de}{dt} \sim 5eB \sqrt{\left(\frac{2B+D}{5B}\right) \left(\sin^2 i_B - \frac{2B+D}{5B}\right)}. \quad (17)$$

In order to increase e , we need $de/dt > 0$, which then leads to

$$0 < 2 + D/B < 5 \sin^2 i_B. \quad (18)$$

This is the condition for Lidov-Kozai effect to operate under the gravity from both binary stars and the disk. For disk-free case, i.e., $D = 0$, then equation (18) is reduced to the classical one, i.e., $i_B > \arcsin(\sqrt{2/5}) \sim 39.2^\circ$.

As D and B are functions of the semimajor axis (a), in equation (18) actually produces two critical semimajor axes, a lower limit of a_{c1} and an upper limit of a_{c2} , which can be derived from $2 + D/B = 0$ and $2 + D/B = 5 \sin^2 i_B$, respectively. If the disk is not very tenuous, such as $f_g > 0.1$, then $S \gg B$ holds and thus equation (16) can be reduced to $D \sim -T - B \cos^2 i_B$. In such a case, we can solve a_{c1} and a_{c2}

⁴ Setting $i_B = 0$ in equations (15) and (16), the binary and disk's contributions to $\frac{d\omega}{dt}$ are $2B$ and $-B - T$ respectively, which are obviously wrong, though their sum ($B - T$) is correct.

analytically if $k = -1$,⁵

$$a_{c1} \sim 4.17 \text{AU} \left[\frac{1}{f_g} \frac{M_B}{M_\odot} (\sin^2 i_B + 1) \right]^{-2/3} \left(\frac{a_B}{50 \text{AU}} \right)^2, \quad (19)$$

$$a_{c2} \sim 4.17 \text{AU} \left[\frac{1}{f_g} \frac{M_B}{M_\odot} (1 - 4 \sin^2 i_B) \right]^{-2/3} \left(\frac{a_B}{50 \text{AU}} \right)^2, \text{ if } i_B < 30^\circ, \\ \sim \infty, \text{ if } i_B \geq 30^\circ. \quad (20)$$

Comparing to the classical disk-free case, where Lidov-Kozai effect takes place only if $i_B > 39.2^\circ$, here Lidov-Kozai effect (or eccentricity excitation) can occur for an arbitrary i_B , and the value of i_B just determines the disk range ($a_{c1} < a < a_{c2}$) that subject to Lidov-Kozai effect.

4. NUMERICAL STUDY

In this section, we perform numerical simulations to test our analytical results presented in section 3. Planetesimals are only subject to the gravity from the binary stars and the disk⁶. We calculate the disk's gravity at lattice points in the r' - z' plane before orbital integrations and obtained the gravitational force at arbitrary point by bicubic interpolation (see the appendix for a detail description about computing disk gravity). The equations of planetesimal motion are integrated using a fourth-order Hermit method (Kokubo et al. 1998).

4.1. Examples

As a first example (hereafter referred to as the standard case), we assume that $M_B = 0.5M_\odot$, $a_B = 50 \text{AU}$, $i_B = 50^\circ$ for the binary and $f_g = 1$, $k = -1$ for the disk. The results of this case is plotted in figure 2 and 3.

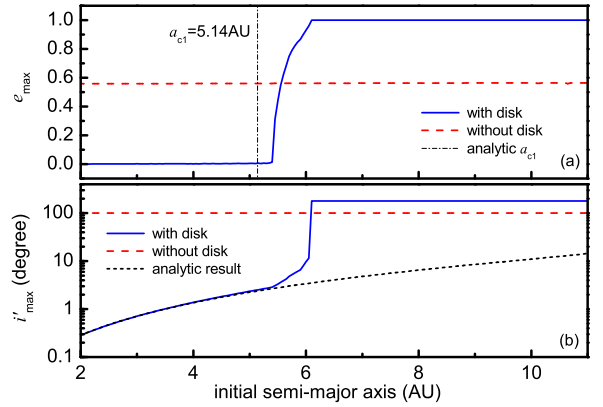


Fig. 2.— Planetesimal's maximum eccentricities (panel (a)) and inclinations (panel (b)) as a function of its initial semi-major axis in the standard case. Red dashed line indicates the results without including disk gravity. In panel (a), the vertical black dash-dotted line indicates the analytical boundary of Kozai effect (Eqn.19). In panel (b), the black dashed line shows the analytical result from equation 13.

⁵ In order to analytically derive a_{c1} and a_{c2} with moderate accuracy, we make the compromise that B and B_1 has the same dependency on a but a little difference in normalization, namely $B = (1 + \eta)B_1$. Here in equation (19) $\eta = 0.4$. Note, equations (19) and (20) cannot be applied to the disk free case by just setting $f_g = 0$ because we have presupposed that $f_g > 0.1$. And for the case of $k \neq -1$, a_{c1} and a_{c2} should be solved numerically from Eqn.18.

⁶ In fact, planetesimals are also subject to the hydrodynamical drag force from the gas disk. See section 5.1 for a discussion of gas drag or see the paper of Xie et al. (2011) for a detailed study of the effects of gas drag.

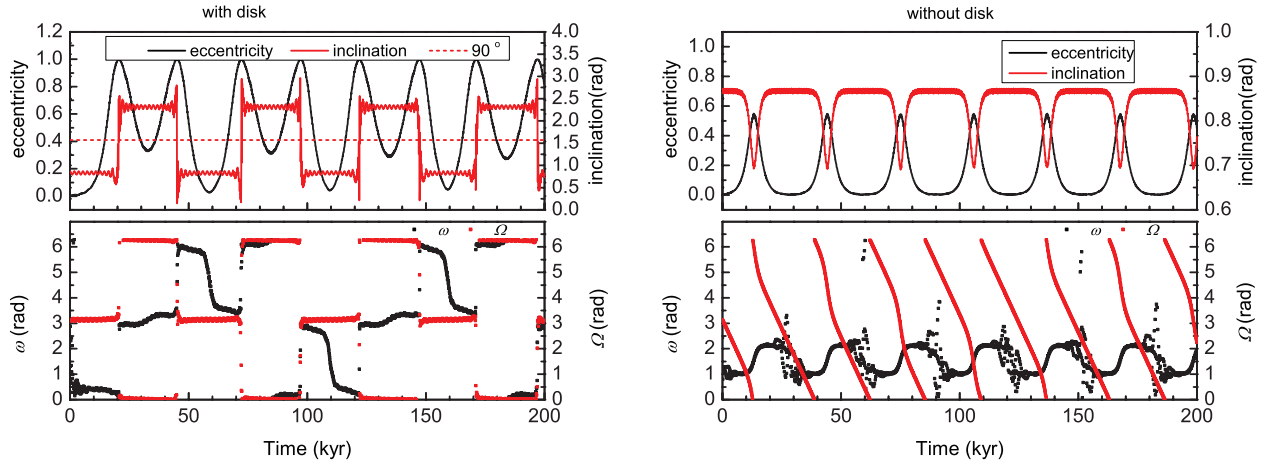


FIG. 3.— Orbital evolution of a planetesimal with semimajor axis at 6.5 AU. All the orbital elements are in the binary coordinate. The two left panels are results of the standard case, while the two right panels are results for the case with the same binary configuration but without including disk gravity. (Note the different scales for the eccentricity and inclination scales in the two plots.)

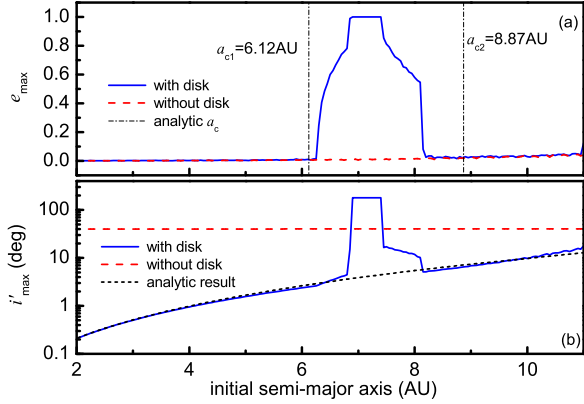


FIG. 4.— Similar to Figure 2 but with $i_B = 20^\circ$

In Figure 2, we plot the maximum orbital eccentricity (e_{max}) and inclination (i'_{max} , in disk coordinates) that the planetesimal achieved during its evolution as a function of its orbital semimajor axis. As can be seen from Figure 2, in the inner region, planetesimal eccentricities are not excited, and they remain at very low inclinations with i'_{max} fitting well with our analytical result (Eqn.13). In the outer region, the Lidov-Kozai effect is switched on, and thus leads to large planetesimal eccentricities ($e_{max} \sim 1$) and inclinations ($i'_{max} > 90^\circ$). The boundary that separates the inner Kozai-off region and the outer Kozai-on region is roughly consistent with the analytical estimate (Eqn.19). In addition, we also plot the results of the disk-free case as shown in the red dashed line in Figure 2. Comparing the two cases of with and without disk, we see that e_{max} is much larger (close to unity) in the former case.

In Figure 3, for a specific planetesimal with semimajor axis of 6.5 AU where the Lidov-Kozai effect should be switched on according to Figure 2, we plot the temporal evolution of its orbital eccentricity (e), inclination (i), longitude of periastron (ω) and ascending node (Ω) for the two cases with and without disk. Note, here all the angular elements plotted in figure 3 are in the binary coordinate. In the case without disk, the two

right panels show the classical ‘‘Lidov-Kozai’’ cycle where the eccentricity and inclination are evolving out of phase. However, the situation is very different if the disk gravity is included in. In such a case, as shown in the two left panels of Figure 3, the planetesimal maintains its orbit around the initial one ($i = i_B, \Omega = 180^\circ$) for a while at the beginning when the eccentricity is not very high. As the planetesimal eccentricity increases to the degree where $e \sim 1$, the planetesimal quickly flips to a retrograde orbit but still in the same plane (the mid-plane of gas disk) with $i \sim \pi - i_B$ and $\Omega = 0$ or π . We note that such an orbital flip as well as the associated high orbital eccentricity is very similar to the one observed recently by Naoz et al. (2011a,b); Lithwick & Naoz (2011), where they assume a non-zero eccentricity of the outer perturbing body, and the orbital flip of the inner body is due to the so-called Eccentric Lidov-Kozai Mechanism (Lithwick & Naoz 2011). While in the present paper, we assume a zero eccentricity of the outer perturbing body ($e_B = 0$), and thus the orbital flip observed in Figure 3 should be due to the effect of disk gravity.

As a second example (hereafter referred to as the low inclination case), we just change the binary orbital inclination to $i_B = 20^\circ$ and keep all the other parameters the same as in the standard case. The result of this low inclination case is plotted in figure 4. In contrast to the $i_B = 50^\circ$ case, here the Lidov-Kozai effect can only take place within the region $a_{c1} < a < a_{c2}$. This is consistent with our analytical results in equations 19 and 20.

4.2. Parameter exploration

In this subsection, we extend the standard case above by numerically investigating the effects of other parameters, including i_B, a_B, M_B, f_g , and k . We adopt the following strategy: To investigate the effect of a given parameter, we set this parameter as the only free one and fix all other parameters as the same as in the standard case. The results are then plotted in Figure 5 and 6. The former shows the radial distribution of planetesimal’s maximum eccentricity and its dependency on i_B (top left), a_B (bottom left), M_B (top right) and f_g (bottom right) in the case of $k = -1$. The latter just shows the dependency on i_B but for the cases of different k values. Some major features can be summarized as the following.

As shown in Figure 5, (1) the Lidov-Kozai effect can be

switched on even with i_B as small as $\sim 5^\circ$, although the width of the Kozai- on region decreases as i_B decreases. (2) The Lidov-Kozai effect can be suppressed over a larger region if either the mass of the companion star decreases, or the separation of the companion and/or the density of the disk increases. (3) The analytical results (dashed and solid lines, see also in Eqn. 19 and 20) approximate the numerical results in the inner region with $a < 9 - 10$ AU. Beyond this, in the region close to the disk outer boundary and the orbital stability boundary, the deviation is large, indicating our analytical approximation is not valid there. And (4) the boundaries that separate the Kozai-on and Kozai-off regions are very steep; most planetesimal eccentricities are either very high (close to 1) or very low (close to 0) with planetesimals of moderate eccentricities being very rare. The effect of the disk density slope k can be seen from Figure 6, which shows (5) the Kozai-off region extends outwards more and more as k increases, i.e., the disk radial density profile becomes more flat. In the case of $k = -1/2$, the Lidov-Kozai effect turns off in the whole disk.

5. DISCUSSION

5.1. Planetesimal Jumping and Pile-up (PJP)

In the early stage, there must be a gas disk around the primary star. The gas disk has crucial effects on the dynamics of planetesimals through two factors. One is the gravity, which was studied in detail in previous sections of this paper. The other one is the hydrodynamic drag force, whose role has been investigated in detail by Xie et al. (2011). In general, Xie et al. (2011) find that if planetesimals are excited to orbits with very high inclinations (relative to the disk plane) and eccentricities, they will be subjected to very strong hydrodynamic drag forces from the gas disk, letting them jump inward and pile up, i.e., the so-called Planetesimal Jumping and Pile-up (PJP) effect. Nevertheless, the disk gravity is not included in by Xie et al. (2011). In the following, we show how the PJP effect is modified if both the gas drag and disk gravity

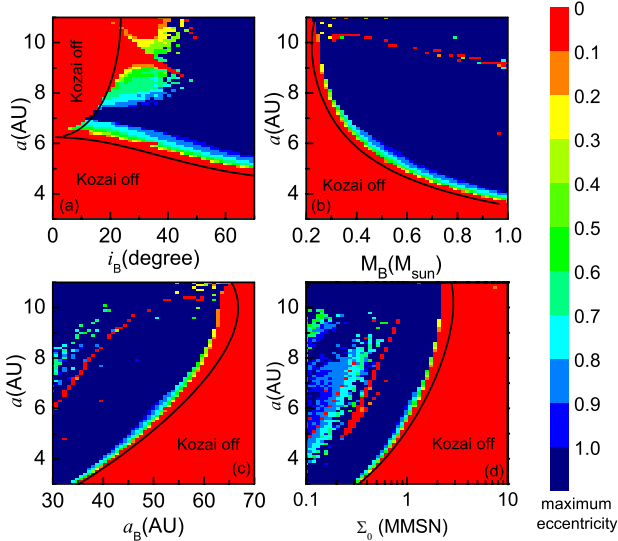


FIG. 5.— Radial distribution of planetesimals' maximum eccentricity and its dependency on i_B (panel a), M_B (panel b), a_B (panel c), and f_g (panel d). Red-color regions mean the planetesimals eccentricities ~ 0 , namely the Lidov-Kozai effect is switched off. The black dashed lines indicate the analytical boundaries of the Lidov-Kozai effect described by Equation 18 For all the four panels, $k = 1$.

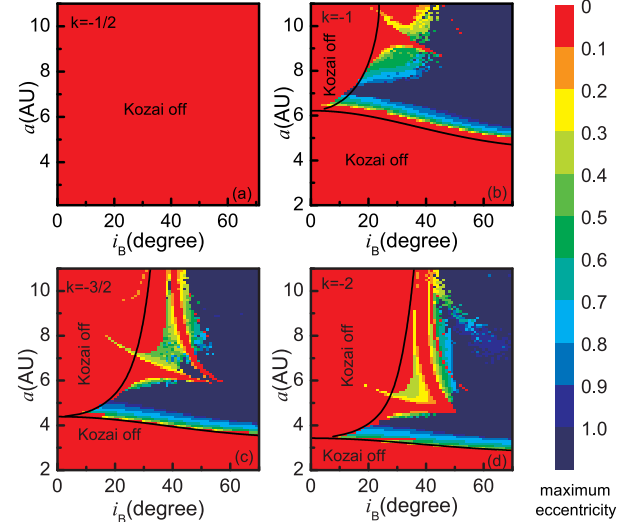


FIG. 6.— Similar to the panel (a) of Figure 5 but for cases of different k values (the disk density slope). As can be seen, a flatter disk tends to be more efficient to suppress the Lidov-Kozai effect. This result is expected as flattening the disk profile is equivalent to increasing the density outside $r = 1$ AU.

are included.

We consider four cases, (a) the standard case as described in section 4.1, (b) a more compact case— similar to the standard case but with a_B decreasing to 40 AU, (c) a low inclination case— similar to the standard case but with i_B decreasing to 20° , and (d) a disk gravity free case— similar to the standard case but the disk gravity is not included. In each case, gas drag force is calculated by assuming a single planetesimal radial size of 5 km and following the procedure as described in section 2.2 of Xie et al. (2011). The results are plotted in figures 7 and 8.

In Figure 7, we plot the evolution of orbital semimajor axis (also periastron, top panel) and eccentricity (bottom panel) of three planetesimals in case (a), i.e., the standard case. Three planetesimals with near circular orbits starting from 5, 6 and

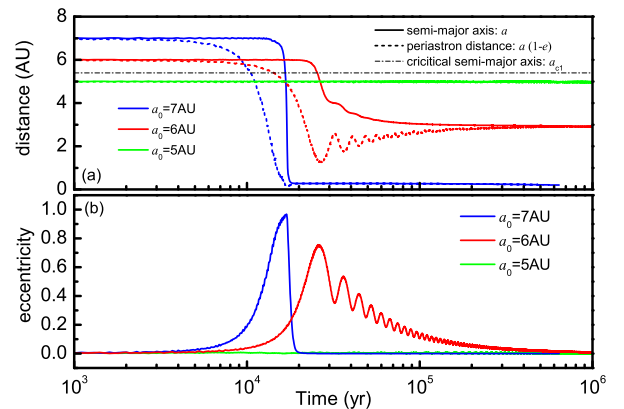


FIG. 7.— Evolution of orbital semimajor axis (also periastron, top panel) and eccentricity (bottom panel) of three planetesimals with initial semimajor axes of 5 (green), 6 (red) and 7 (blue) AU respectively. The binary configuration is set as in the standard case described in section 4.1 but adding in the gas drag. The black dashed-dot line denotes the critical semimajor axis $a_{c1} = 5.4$ AU as measured from Figure 2.

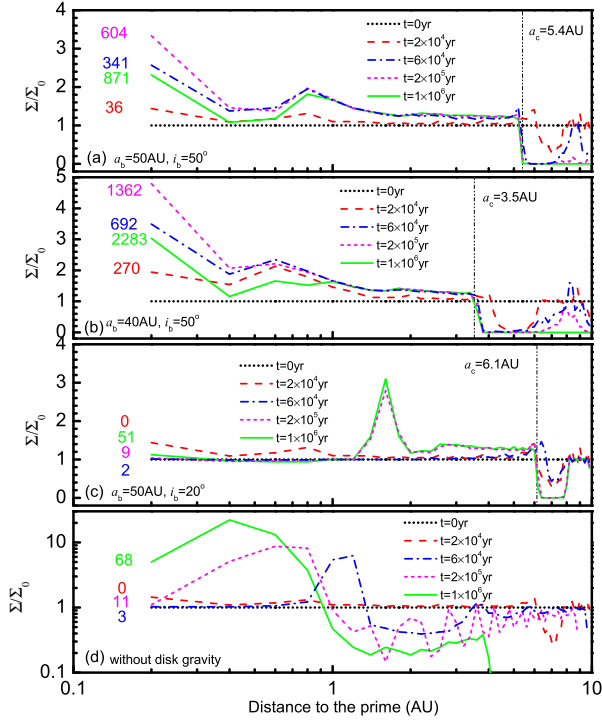


FIG. 8.— Evolution of the local surface density enhancement (Σ/Σ_0) of the planetesimal disk in the standard case (a), compact case (b), small inclination case (c) and the disk gravity free case (d). The vertical black dash-dotted lines show the critical semi-major axis that separate the Kozai-on and Kozai-off regions. The number on the left of each profile curve denotes the total number of planetesimals which have migrated to the innermost region within 0.2 AU. Note the scale of the vertical axis is different in the bottom panel as compared to those in the others.

7 AU. Beyond $a_c = 5.4$ AU, where the Lidov-Kozai effect is switched on, the two planetesimals’ eccentricities are excited and thus they suffer significant gas drag force, leading to rapid inward migration. The one starting from 7 AU is excited to extremely high eccentricity and directly jumps to the innermost orbit, and the one starting from 6 AU with modest eccentricity quickly migrates to 2-3 AU the central star. On the other side, for $a_c < 5.4$ AU, the Lidov-Kozai effect is suppressed, and thus the planetesimal starting from 5 AU does not suffer eccentricity excitation and hence does not migrate.

In Figure 8, we plot the evolution of the local surface density enhancement (Σ/Σ_0) of the planetesimal disk for the four cases. In each case, 5000 planetesimals treated as test particle tracers, are initially distributed uniformly from 0.2 AU to 10 AU in the mid-plane of gas disk with circular orbits, thus the initial profile follows a power law with a semi-major axis dependence equal to -1 . By tracing the radial distribution of those planetesimals, we can calculate the local surface density enhancement (Σ/Σ_0) of the planetesimal disk. The results are shown in Figure 8 and can be summarized as follows:

(1) As can be seen in the top panel (case a), planetesimals in the outer Kozai-on region migrate into the inner Kozai-off region (in fact, most are “jumping” as shown in Figure. 7 and pile up there, leading to surface density enhancement in the innermost region ($a < 0.2$ AU). This pile-up effect increases when the binary separation, a_B , decreases (case b), because the outer Kozai-on region is larger and thus more planetesi-

imals can move in and pile up. Conversely, when we reduce i_B (case c), the pile-up effect is reduced, and the pile-up region shifts outward to 1- 2 AU, because the outer Kozai-on region shrinks and less particles are excited to eccentricity close to 1 (see Figure. 4).

(2) If the disk gravity is not included (case d), then the situation reduces to the situation considered in Xie et al. (2011). In such a case, the Lidov-Kozai effect can only be suppressed by the gas damping and this only in the very inner region within 1-2 AU, where gas density is high. Beyond 1-2 AU, planetesimals experience the Lidov-Kozai effect and most (if not all) will migrate inward and pile up within $\sim 0.2 - 1.0$ AU, leading to an average local density enhancement of $\Sigma/\Sigma_0 \sim 10$ (see also in the Figure. 9 of Xie et al. (2011)). However, we note that there are many fewer planetesimals piling up within region < 0.2 AU in case (d) than in case (a). The reason is that the planetesimal eccentricity (see Figure. 3) in case (d) is not high enough to let planetesimals directly jump into the innermost region < 0.2 AU.

In a word, the role of the disk gravity playing in the PJP effect can be summarized as the following. On one hand, disk gravity reduces the average PJP effect because it reduces the Kozai-on region in the outer disk. However, on the other hand, the disk gravity significantly enhances the PJP effect in the innermost region (< 0.2 AU) as it increases the orbital eccentricities of planetesimals in the Kozai-on region to values close to 1.

5.2. Effects of Planetesimal Collisions

In this paper, the planetesimals are treated as test particles and their mutual collisions are ignored. As planetesimals jump inward, their orbital eccentricities are very high and thus they are potentially subject to collisions of very high relative velocities, which can entirely disrupt themselves. To know how relevant the collisions could be, we estimate the collisional timescale (t_{col}) first. Following Xie et al. (2010b), t_{col} in an inclined binary system can be estimated as ⁷.

$$t_{col} \sim \frac{4}{3} \times 10^4 f_g^{-1} f_{ice}^{-1} \left(\frac{i_B}{1^\circ}\right) \left(\frac{a}{\text{AU}}\right)^3 \left(\frac{M_A}{M_\odot}\right)^{-1/2} \left(\frac{R_p}{\text{km}}\right) \text{ yr}, \quad (21)$$

where f_{ice} is solid density enhancement beyond the ice line, R_p is the planetesimal radii. Taking typical parameters, i.e., $f_g = 1.0, f_{ice} = 4.2, i_B = 50^\circ, M_A = M_\odot, R_p = 5$ km, it gives $t_{col} \sim 8 \times 10^5 (a/\text{AU})^3$ yr. As planetesimals complete their jumps typically in a timescale of $10^4 - 10^5$ yr shown in Figure 7 and 8, thus we conclude that collisions have little effects before or under the process of planetesimal jumping, but they do play important roles after planetesimals jumping inside 1 AU. Actually, this expectation is confirmed by the simulations in Xie et al. (2011). As shown in the figure 13 of their paper, in the first 10 yr, the collisional velocity is very high but the collisional frequency is rather low. Afterwards, collisions become more frequent as more planetesimals pile up in the inner region. At the same time, planetesimals are damped to near coplanar and circular orbits, leading to a friendly condition for subsequent planetesimal growth by mutual collisions.

5.3. Implication to the Formation of Hot Jupiters

The Lidov-Kozai effect induced by a companion star in a binary system has been suggested as an important mechanism for the formation of hot Jupiters (Wu & Murray 2003;

⁷ Combine Eqn (3), (6) and (7) in Xie et al. (2010b)

Fabrycky & Tremaine 2007). If a planet’s eccentricity is high enough that its periastron is very close to the star (say < 0.1 AU) during the Kozai cycle, then tidal dissipation can kick in, which may circularize and shrink the planet’s orbit, finally letting it become a hot planet. However, to induce such a high eccentricity by the classical Lidov-Kozai effect, it needs an extremely misaligned configuration⁸ (say $i_B > 85^\circ$, according to Wu & Murray (2003)), which is not common and thus lowers the chance of forming a hot-Jupiter. As estimated by Wu et al. (2007), such a “stellar Kozai” mechanism can only produce 10% hot Jupiters.

Nevertheless, the situation will be different if the disk gravity is included in the Lidov-Kozai effect. In such an case, almost in the whole Kozai-on region, the eccentricity can be excited to be an arbitrarily high value even with very low initial binary inclination (i_B), which produces many more “hot planetsimals” ($a < 0.2$ AU) as shown in Figure 8. Similarly, if our model and results can be applied to a Jupiter-like planet⁹ (by replacing the gas drag damping with tidal damping in figure 8), it should also produce many more hot Jupiters. The key issue is, to what degree the production rate of hot jupiter can increase via the above “modified stellar Kozai” mechanism. We will address this in detail in a forthcoming paper.

5.4. Disk Precession

In this paper, we assume that the gas disk is non-evolving and axisymmetric, which is apparently a crude approximation. In fact, the gas disk (if it is not entirely disrupted) should undergo a near rigid body precession (Larwood et al. 1996; Fragner & Nelson 2010), and the precession rate can be estimated as

$$\dot{\Omega}_d = - \left(\frac{3GM_B}{4a_B^3} \cos i_B \frac{\int \Sigma_g r^3 dr}{\int \Sigma_g \Omega_{k,\text{mid}} r^3 dr} \right). \quad (22)$$

For the standard case considered in this paper, equation 22 gives $\dot{\Omega}_d \sim -2.6 \times 10^{-4} \text{ rad yr}^{-1}$. Adding such a rigid precession to the gas disk, we re-run the simulations shown in the top-left panel of Figure 5 and plot the results in Figure 9. The two black solid curves in Figure 9 are two critical semimajor axes (a_{c1} and a_{c2}) derived from equation 18 (not from Eqn.19 and 20) by assuming

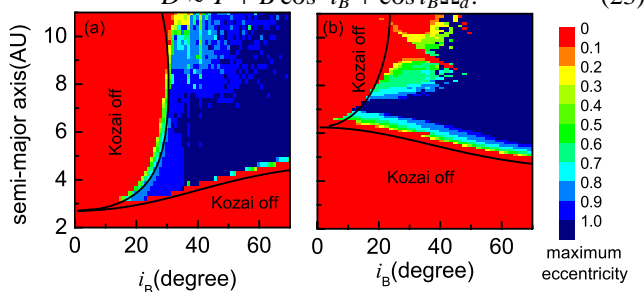
$$D \approx T + B \cos^2 i_B + \cos i_B \dot{\Omega}_d. \quad (23)$$


Fig. 9.— Panel (a). Maximum eccentricities distribution in the plane of $i_B - a$ if the precession of the disk is considered. The black solid lines indicate the analytic boundaries of Kozai-on region. Panel (b). Same as the top left panel of Fig 5. Maximum eccentricities distribution if the precession of the disk is not considered.

⁸ The critical i_B can be lower if one considers the effect of the binary eccentricity (Lithwick & Naoz 2011)

⁹ Note, the results might be different because the giant planet can significantly affect the gas disk, e.g., opening a gap.

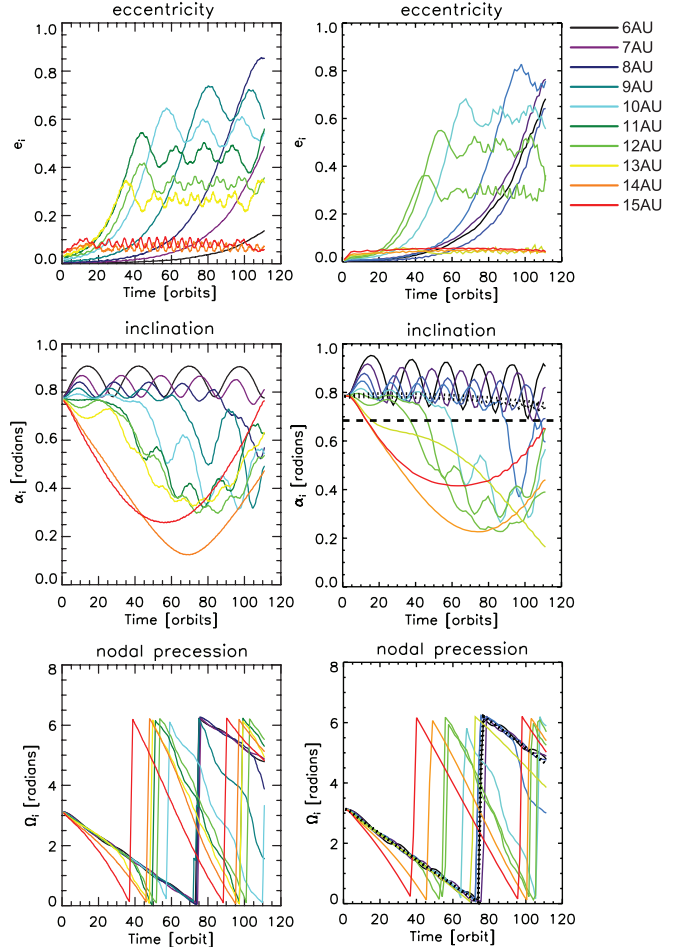


Fig. 10.— Comparison between our results (left three panels) and those in figure 10 of Fragner et al. (2011) (right three panels). From top to bottom, they are evolutions of planetesimals’ eccentricities, orbital inclinations (relative to the binary orbital plane), and nodal precession, respectively. The line color indicate the planetesimal’s initial semi-major axis. The initial setup, including the configuration of the binary and disk is adopted from the model 3 of Fragner et al. (2011) (see section 3.2 and table 2 of their paper).

Although equation 23 is a very crude approximation, it produces reasonable a_{c1} and a_{c2} which fit the numerical results as well as shown in Figure 9. Furthermore, both the cases with and without disk precession (comparing the two panels of Fig.9) produce some similar features, such as: (i) in the central regions of the disk, the Lidov-Kozai effect can be switched on at very low inclinations, and (ii) once the Lidov-Kozai effect is switched on, the planetesimal eccentricities can be much higher (most are close to 1) than those in the case without disk gravity.

5.5. Comparison to the Hydrodynamical Results

In order to further examine the validity of our disk model, we compare the results of our model to the hydrodynamical results given by Fragner et al. (2011). We adopt the same initial set up as in the simulations shown in the figure 10 of Fragner et al. (2011) and run the simulation with our model and numerical method described in Appendix D. The comparison results are plotted in Figure 10. As can be seen, the results computed by our model are generally consistent with the hydrodynamical results of Fragner et al. (2011). Given such a comparison, we then feel confident of the results shown in

other places of this paper.

6. SUMMARY

In this paper, we investigated the effects of gas-disk gravity on planetesimal dynamics in inclined binary systems using both analytic and numerical methods. Our major conclusions are summarized as the following.

Analytically, we derive that the planetesimal inclination follows a small amplitude oscillation around the mid-plane of disk (see Eqn.12 and 13) if the Lidov-Kozai effect is suppressed and thus planetesimal eccentricity is not excited. Furthermore, we derive the threshold condition (see Eqn.18, 19 and 20) in which the Lidov-Kozai effect switches on. We find the Lidov-Kozai effect can operate at very low inclinations if the disk gravity is considered, although the radial extent of the Kozai-on region is much smaller.

Numerically, we confirm our analytical results over a very large parameter space by considering the variation of i_B , a_B , M_B , f_g . We find that the disk gravity narrows down the Kozai-on region, but at the same time significantly increases the maximum eccentricity (close to 1) of planetesimals in the

Kozai-on region (see Figure 2). Such high planetesimal eccentricities usually accompany orbital flipping (see Figure 3), i.e., planetesimal orbits flip back and forth between prograde to retrograde.

Applying the effects of disk gravity to the planetesimal jumping-piling (PJP) process. We find that, on the average over the disk, disk gravity reduces the PJP effect. However, PJP effect is significantly enhanced in the innermost region within 0.2 AU (see Figure 8). In addition, given the extremely high eccentricity under the effects of disk gravity, we believe that the production rate of hot-Jupiters via the ‘‘stellar Kozai’’ mechanism could be increased.

We are grateful to Dr. Matthew Payne, Dr. Sverre Aarseth and Dr. Yanqin Wu for useful discussions and suggestions. This work is supported by the National natural Science Foundation of China (Nos.10833001, 10778603, and 10925313), and the National Basic Research Program of China(No.2007CB814800).

APPENDIX

A. THE DISTURBING FUNCTION OF THE DISK

According to Nagasawa et al. 2000, taken to second order in e and i' , the disturbing function caused by the disk can be expressed as

$$R_D = -\frac{na^2}{2} [T(a)e^2 + S(a)i'^2], \quad (\text{A1})$$

$T(a)$ and $S(a)$ are given using an integral of cylindrical coordinates (r', ϕ', z') :

$$\begin{aligned} T(a) &= \frac{1}{2n} \int_{r_{\text{in}}}^{r_{\text{out}}} \int_{-\infty}^{\infty} \int_0^{2\pi} \left[\frac{3 - 2r' \cos \phi' / a}{\Delta^3} \right. \\ &\quad \left. - \frac{3(a - r' \cos \phi')^2}{\Delta^5} \right] G\rho_g(r', z') r' dr' d\phi' dz', \\ S(a) &= \frac{1}{2n} \int_{r_{\text{in}}}^{r_{\text{out}}} \int_{-\infty}^{\infty} \int_0^{2\pi} \left(\frac{r' \cos \phi' / a}{\Delta^3} - \frac{3z'^2}{\Delta^5} \right) G\rho_g(r', z') r' dr' d\phi' dz', \end{aligned} \quad (\text{A2})$$

where $\Delta = (a^2 + r'^2 + z'^2 - 2ar' \cos \phi')^{1/2}$

B. INCLINATION EVOLUTION EQUATION

Ignoring e^2 and higher order terms in the disturbing function R , perturbation function relating to the inclination has the form

$$R = \frac{na^2}{2} [-S(a)i'^2 - B(a) \sin^2 i], \quad (\text{B1})$$

where i is the inclination in the binary coordinate and i' is that in the disk coordinate. In the binary coordinate system, the xy-plane is the binary's orbital plane, and the x-axis is the ascending node of the companion with respect to the disk. In the coordinate system of the disk, the x-axis is same as that of the binary coordinate system, and the xy-plane is the mid-plane of the disk.

According to the geometrical relationship between the two coordinate, we have

$$\begin{pmatrix} \sin i \sin \Omega \\ -\sin i \cos \Omega \\ \cos i \end{pmatrix} = \begin{pmatrix} 1 & 0 & 0 \\ 0 & \cos i_B & \sin i_B \\ 0 & -\sin i_B & \cos i_B \end{pmatrix} \begin{pmatrix} \sin i' \sin \Omega' \\ -\sin i' \cos \Omega' \\ \cos i' \end{pmatrix}. \quad (\text{B2})$$

It is easy to obtain

$$\begin{cases} \sin i \sin \Omega &= \sin i' \sin \Omega', \\ \sin i \cos \Omega &= \sin i' \cos \Omega' \cos i_B - \cos i' \sin i_B, \\ \cos i &= \sin i' \cos \Omega' \sin i_B + \cos i' \cos i_B. \end{cases} \quad (\text{B3})$$

Then

$$\begin{aligned}
\sin^2 i &= 1 - \sin^2 i' \cos^2 \Omega' \sin^2 i_B - \cos^2 i' \cos^2 i_B - 2 \sin i' \cos \Omega' \sin i_B \cos i' \cos i_B \\
&= \sin^2 i_B + \sin^2 i' \cos^2 i_B - \sin^2 i' \cos^2 \Omega' \sin^2 i_B - \sin i' \cos i' \cos \Omega' \sin 2i_B \\
&= \sin^2 i_B + \sin^2 i' \sin^2 \Omega' \cos^2 i_B + \sin^2 i' \cos^2 \Omega' \cos 2i_B - \sin i' \cos i' \cos \Omega' \sin 2i_B \\
&= i'^2 \sin^2 \Omega' \cos^2 i_B + i'^2 \cos^2 \Omega' \cos 2i_B - i' \cos \Omega' \sin 2i_B + \sin^2 i_B + o(i'^3).
\end{aligned} \tag{B4}$$

If we ignore i^3 and higher order terms, the relationship becomes

$$\sin^2 i = p^2 \cos^2 i_B + q^2 \cos 2i_B - q \sin(2i_B) + \sin^2 i_B, \tag{B5}$$

where $p = i' \sin \Omega'$ and $q = i' \cos \Omega'$. Thus the perturbation function becomes

$$R = \frac{na^2}{2} \left[-(B \cos^2 i_B + S)p^2 - (S + B \cos 2i_B)q^2 + B \sin(2i_B)q - B \sin^2 i_B \right] \tag{B6}$$

Using Lagrange's equations of motion, the evolution of the inclination is given by

$$\begin{aligned}
\frac{dp}{dt} &= -(B \cos 2i_B + S)q + \frac{B}{2} \sin(2i_B), \\
\frac{dq}{dt} &= (B \cos^2 i_B + S)p.
\end{aligned} \tag{B7}$$

C. THE CONTRIBUTION OF DISK TO THE PERIASTRON PRECESSION

The disturbing function of the disk has the form

$$R_D = -\frac{na^2}{2} \left[T(a)e^2 + S(a)i'^2 \right]. \tag{C1}$$

Using Lagrange's equations of motion, and ignoring the e^2 term, we can the expression for the evolution of ω cause by the disk

$$\left(\frac{d\omega}{dt} \right)_{\text{disk}} = -T + \frac{1}{2} S \cot i (\partial i'^2 / \partial i) \equiv D. \tag{C2}$$

where i and i' are the inclinations in the companion coordinate system and disk coordinate system. Proceeding with the same method as used in Appendix A, we have

$$\sin^2 i' = \sin^2 i \sin^2 \Omega \cos^2 i_B + \sin^2 i \cos^2 \Omega \cos 2i_B + \sin i \cos i \cos \Omega \sin 2i_B + \sin^2 i_B, \tag{C3}$$

then we can obtain that

$$\begin{aligned}
\partial(\sin^2 i') / \partial i &= \sin 2i \sin^2 \Omega \cos^2 i_B + \sin 2i \cos^2 \Omega \cos 2i_B + \cos 2i \cos \Omega \sin 2i_B \\
&= 2 \cot i \left(\sin^2 i \sin^2 \Omega \cos^2 i_B + \sin^2 i \cos^2 \Omega \cos 2i_B + \sin i \cos i \cos \Omega \sin 2i_B + \sin^2 i_B \right) - \cos \Omega \sin 2i_B - 2 \cot i \sin^2 i_B \\
&= \left[2 \sin^2 i' \cos i - 2 \sin i_B (\sin i \cos \Omega \cos i_B + \cos i \sin i_B) \right] / \sin i \\
&= \left(2 \sin^2 i' \cos i - 2 \sin i' \cos \Omega' \sin i_B \right) / \sin i.
\end{aligned} \tag{C4}$$

Because initially $i' = 0$, we ignore $o(i'^2)$ term and have

$$\partial(i'^2) / \partial i = -2i' \cos \Omega' = -2q. \tag{C5}$$

We have obtained previously that

$$q = i' \cos \Omega' = \frac{B \sin(2i_B)}{2B \cos 2i_B + 2S} [1 - \cos(ft)]. \tag{C6}$$

For the case $S \gg B$, the timescale of the evolution of i' and Ω' is much shorter than the Kozai timescale. Thus we replace q with its average value

$$\langle q \rangle = \frac{B \sin(2i_B)}{2B \cos 2i_B + 2S} = i'_{\max} / 2. \tag{C7}$$

and D becomes

$$D = -T - \frac{1}{2} S i_{\max} \cot i = -T - \frac{SB \cos^2 i_B}{(B \cos 2i_B + S)}. \tag{C8}$$

D. GRAVITATIONAL FORCE OF THE DISK

According to Nagasawa et al. (2000), the potential of the disk at (r, ϕ, z) is

$$V = G \int_{r_{\text{in}}}^{r_{\text{out}}} \int_{-\infty}^{\infty} \int_0^{2\pi} \frac{\rho(r', z') r' d\phi' dz' dr'}{(r^2 + r'^2 - 2rr' \cos \phi' + (z - z')^2 + \epsilon)^{1/2}}, \quad (\text{D1})$$

where r_{in} , and r_{out} are the inner edge and the outer edge of the disk, respectively, and ϵ is a softening parameter used to avoid a singularity. For reasons of efficiency and precision, we set it to be 1×10^{-7} . Derivative of the potential with respect to r or z yields the r or z component of the disks gravity,

$$\begin{aligned} F_r &= G \int_{r_{\text{in}}}^{r_{\text{out}}} \int_{-\infty}^{\infty} \int_0^{2\pi} \frac{\rho(r', z')(r - r' \cos \phi') r' d\phi' dz' dr'}{(r^2 + r'^2 - 2rr' \cos \phi' + (z - z')^2 + \epsilon)^{3/2}}, \\ F_z &= G \int_{r_{\text{in}}}^{r_{\text{out}}} \int_{-\infty}^{\infty} \int_0^{2\pi} \frac{\rho(r', z')(z - z') r' d\phi' dz' dr'}{(r^2 + r'^2 - 2rr' \cos \phi' + (z - z')^2 + \epsilon)^{3/2}}, \end{aligned} \quad (\text{D2})$$

We numerically integrated equation (D2) using closed Newton-Cotes formulas with Bodes rule (Press et al. 1992). Since the integration costs too much CPU time, we can not do it for each orbital integration step. Instead, we calculated the disks gravity at lattice points in the r - z plane before starting the orbital integrations and obtained the gravitational force at arbitrary points during the orbital integration by performing bicubic interpolations (Press et al. 1992) using the value at lattice points.

REFERENCES

- Artymowicz, P., & Lubow, S. H. 1994, *ApJ*, 421, 651
 Batygin, K., Morbidelli, A., & Tsiganis, K. 2011, *A&A*, 533, A7
 Beaugé, C., Leiva, A. M., Haghighipour, N., & Otto, J. C. 2010, *MNRAS*, 408, 503
 Chauvin, G., Beust, H., Lagrange, A.-M., & Eggenberger, A. 2011, *A&A*, 528, A8
 Eggenberger, A. 2010, *EAS Publications Series*, 42, 19
 Fabrycky, D., & Tremaine, S. 2007, *ApJ*, 669, 1298
 Fragner, M. M., & Nelson, R. P. 2010, *A&A*, 511, A77
 Fragner, M. M., Nelson, R. P., & Kley, W. 2011, *A&A*, 528, A40
 Correia, A. C. M., et al. 2008, *A&A*, 479, 271
 Giuppone, C. A., Leiva, A. M., Correa-Otto, J., & Beaugé, C. 2011, *A&A*, 530, A103
 Haghighipour, N. 2010, *EAS Publications Series*, 42, 365
 Hale, A. 1994, *AJ*, 107, 306
 Hatzes, A. P., Cochran, W. D., Endl, M., McArthur, B., Paulson, D. B., Walker, G. A. H., Campbell, B., & Yang, S. 2003, *ApJ*, 599, 1383
 Hayashi, C. 1981, *Progress of Theoretical Physics Supplement*, 70, 35
 Heppenheimer, T. A. 1978, *A&A*, 65, 421
 Innanen, K. A., Zheng, J. Q., Mikkola, S., & Valtonen, M. J. 1997, *AJ*, 113, 1915
 Jensen, E. L. N., Mathieu, R. D., Donar, A. X., & Dullighan, A. 2004, *ApJ*, 600, 789
 Katz, B., & Dong, S. 2011, *arXiv:1105.3953*
 Katz, B., Dong, S., & Malhotra, R. 2011, *Physical Review Letters*, 107, 181101
 Kley, W., & Nelson, R. P. 2008, *A&A*, 486, 617
 Kokubo, E., Yoshinaga, K., & Makino, J. 1998, *MNRAS*, 297, 1067
 Kozai, Y. 1962, *AJ*, 67, 591
 Larwood, J. D., Nelson, R. P., Papaloizou, J. C. B., & Terquem, C. 1996, *MNRAS*, 282, 597
 Lidov, M. L. 1962, *Planet. Space Sci.*, 9, 719
 Lin, D. N. C., Bodenheimer, P., & Richardson, D. C. 1996, *Nature*, 380, 606
 Lithwick, Y., & Naoz, S. 2011, *ApJ*, 742, 94
 Marzari, F., & Scholl, H. 2000, *ApJ*, 543, 328
 Marzari, F., Thébault, P., & Scholl, H. 2009, *A&A*, 507, 505
 Moriwaki, K., & Nakagawa, Y. 2004, *ApJ*, 609, 1065
 Mugrauer, M., & Neuhäuser, R. 2009, *A&A*, 494, 373
 Nagasawa, M., Tanaka, H., & Ida, S. 2000, *AJ*, 119, 1480
 Naoz, S., Farr, W. M., Lithwick, Y., Rasio, F. A., & Teysandier, J. 2011, *Nature*, 473, 187
 Naoz, S., Farr, W. M., Lithwick, Y., Rasio, F. A., & Teysandier, J. 2011, *arXiv:1107.2414*
 Paardekooper, S.-J., Thébault, P., & Mellema, G. 2008, *MNRAS*, 386, 973
 Paardekooper, S.-J., & Leinhardt, Z. M. 2010, *MNRAS*, 403, L64
 Press, W. H., Teukolsky, S. A., Vetterling, W. T., & Flannery, B. P. 1992, *Cambridge: University Press*, —c1992, 2nd ed.,
 Queloz, D., et al. 2000, *A&A*, 354, 99
 Scholl, H., Marzari, F., & Thébault, P. 2007, *MNRAS*, 380, 1119
 Takeuchi, T., & Lin, D. N. C. 2002, *ApJ*, 581, 1344
 Thébault, P., Marzari, F., Scholl, H., Turrini, D., & Barbieri, M. 2004, *A&A*, 427, 1097
 Thébault, P., Marzari, F., & Scholl, H. 2006, *ICARUS*, 183, 193
 Thébault, P., Marzari, F., & Scholl, H. 2008, *MNRAS*, 388, 1528
 Thébault, P., Marzari, F., & Scholl, H. 2009, *MNRAS*, 393, L21
 Thébault, P. 2011, *Celestial Mechanics and Dynamical Astronomy*, 25
 Trilling, D. E., Lunine, J. I., & Benz, W. 2002, *A&A*, 394, 241
 Weidenschilling, S. J., & Davis, D. R. 1985, *ICARUS*, 62, 16
 Whitmire, D. P., Matese, J. J., Criswell, L., & Mikkola, S. 1998, *ICARUS*, 132, 196
 Wu, Y., & Murray, N. 2003, *ApJ*, 589, 605
 Wu, Y., Murray, N. W., & Ramsahai, J. M. 2007, *ApJ*, 670, 820
 Xie, J.-W., & Zhou, J.-L. 2008, *ApJ*, 686, 570
 Xie, J.-W., & Zhou, J.-L. 2009, *ApJ*, 698, 2066
 Xie, J.-W., Payne, M. J., Thébault, P., Zhou, J.-L., & Ge, J. 2010, *ApJ*, 724, 1153
 Xie, J.-W., Zhou, J.-L., & Ge, J. 2010, *ApJ*, 708, 1566
 Xie, J.-W., Payne, M. J., Thébault, P., Zhou, J.-L., & Ge, J. 2011, *ApJ*, 735, 10
 Zucker, S., Mazeh, T., Santos, N. C., Udry, S., & Mayor, M. 2004, *A&A*, 426, 695